ELSEVIER

Journal of Organometallic Chemistry 562 (1998) 17–27

Journal of Organometallic Chemistry

Synthesis, crystal structure and some reactions of the ruthenacarborane complex $[Ru(CO)_2(MeC{\equiv}CPh)(\eta^5\text{-}7,8\text{-}C_2B_9H_{11}]$[1,2]

John C. Jeffery [a], Paul A. Jelliss [b], Elefteria Psillakis [a], Gillian E.A. Rudd [b], F. Gordon A. Stone [b,*]

[a] *School of Chemistry, The University of Bristol, Bristol BS8 1TS, UK*
[b] *Department of Chemistry, Baylor University, Waco, TX 76798-7348, USA*

Received 11 May 1997

Abstract

The alkyne complex $[Ru(CO)_2(MeC{\equiv}CPh)(\eta^5\text{-}7,8\text{-}C_2B_9H_{11}]$ (**3c**) has been prepared and its structure determined by X-ray crystallography. The ruthenium is co-ordinated on one side by the *nido*-7,8-$C_2B_9H_{11}$ fragment in a pentahapto manner, and on the other by the two CO molecules and the alkyne [Ru–$C_{av.}$ = 2.305, C–C = 1.228(3) Å. Treatment of **3c** with PEt_3 and $Ph_2PCH_2PPh_2$ in CH_2Cl_2 affords the ylid complexes $[Ru\{C(Me){=}C(Ph)PEt_3\}(CO)_2(\eta^5\text{-}7,8\text{-}C_2B_9H_{11})]$ (**4b**) and $[Ru\{C(Me){=}C(Ph)P(Ph)_2CH_2PPh_2\}(CO)_2(\eta^5\text{-}7,8\text{-}C_2B_9H_{11})]$ (**4c**), respectively. The structure of **4b** was established by an X-ray diffraction study which revealed that the PEt_3 molecule was attached to the carbon atom of the CPh group. In contrast, reactions between **3c** and the donor molecules $AsPh_3$, $SbPh_3$ and $Ph_2P(S)CH_2P(S)Ph_2$ resulted in displacement of the alkyne and formation of the complexes $[Ru(CO)_2(L)(\eta^5\text{-}7,8\text{-}C_2B_9H_{11})]$ (**5a**, L = $AsPh_3$; **5b**, L = $SbPh_3$; **5c**, L = $Ph_2P(S)CH_2P(S)Ph_2$). Treatment of **4c** with the $Ru(CO)_2(\eta^5\text{-}7,8\text{-}C_2B_9H_{11})$ fragment yielded the diruthenium complex $[Ru_2(\mu\text{-}Ph_2PCH_2PPh_2)(CO)_4(\eta^5\text{-}7,8\text{-}C_2B_9H_{11})_2]$ (**6**). The structure, based on the linking of two $Ru(CO)_2(\eta^5\text{-}7,8\text{-}C_2B_9H_{11})$ groups by the ligand $Ph_2PCH_2PPh_2$, was determined by X-ray crystallography. NMR data for the new complexes are reported.

Keywords: Boron; Carborane; Ruthenium; Alkyne

1. Introduction

We have previously reported a high yield synthesis of the complex $[Ru(CO)_3(\eta^5\text{-}7,8\text{-}C_2B_9H_{11})]$ (**1**) ([1]a). Treatment of the latter with $[NEt_4]I$ affords the salt $[NEt_4][RuI(CO)_2(\eta^5\text{-}7,8\text{-}C_2B_9H_{11})]$ which reacts with $AgBF_4$ in THF (tetrahydrofuran) to give $[Ru(CO)_2(THF)(\eta^5\text{-}7,8\text{-}C_2B_9H_{11})]$ (**2**). Complexes **1** and **2** are isolobal with the long known and synthetically useful species $[Mn(CO)_3(\eta^5\text{-}C_5H_5)]$ and $[Mn(CO)_2(THF)(\eta^5\text{-}C_5H_5)]$, respectively, and we have been able to employ them as precursors to a variety of other ruthenacarborane compounds [1]. Thus the THF molecule in **2** is readily substituted by MeC≡CMe or PhC≡CPh to yield alkyne complexes $[Ru(CO)_2(RC{\equiv}CR)(\eta^5\text{-}7,8\text{-}C_2B_9H_{11})]$ (**3a**, R = Me; **3b**, R = Ph).

A feature of the chemistry of complexes **3a** and **3b**, which formally involve Ru^{II} centres, is their apparent ready reaction with nucleophiles ([1]b). For example, **3a** with PPh_3 gives the ylid complex $[Ru\{C(Me){=}C(Me)PPh_3\}(CO)_2(\eta^5\text{-}7,8\text{-}C_2B_9H_{11})]$ (**4a**).

* Corresponding author. E-mail: Gordon_Stone@baylor.edu

[1] Dedicated to my (FGAS) student Professor R. Bruce King on the occasion of his 60th birthday.

[2] The ruthenacarboranes described in this article have icosahedral frameworks with *closo*-1,2-dicarba-3-ruthenadodecaborane structures. However, in the formulae we represent the cages as a *nido*-11-vertex ligand with numbering as for an icosahedron from which the twelfth vertex has been removed. This emphasises the pentahapto ligating character of these groups with the cage acting formally as a four electron donor to the ruthenium centre and being thus related to the five-electron donor $\eta^5\text{-}C_5H_5$.

0022-328X/98/$19.00
PII S0022-328X(98)00363-5

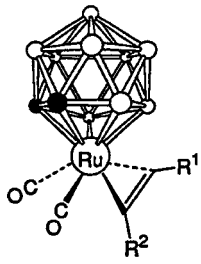

	R^1	R^2
3a	Me	Me
3b	Ph	Ph
3c	Me	Ph

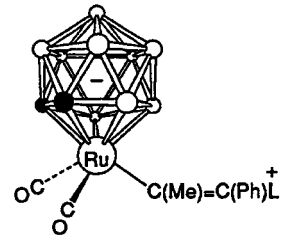

	L
4b	PEt_3
4c	$PPh_2CH_2PPh_2$

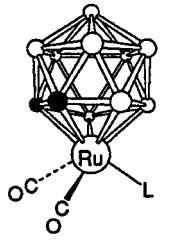

	L
5a	$AsPh_3$
5b	$SbPh_3$
5c	$S=P(Ph_2)CH_2P(Ph_2)=S$

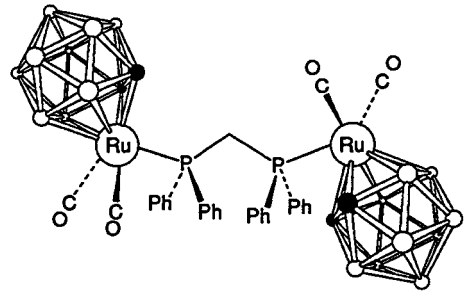

6

● CH ○ BH

Scheme 1.

In this paper we report the synthesis of the alkyne complex $[Ru(CO)_2(MeC{\equiv}CPh)(\eta^5\text{-}7,8\text{-}C_2B_9H_{11})]$ (**3c**) and studies of its reactions with some donor molecules. The object of the study was 2-fold. The presence of the unsymmetrical alkyne in **3c** raises the question as to which ligated carbon atom is the preferred site of attachment by a donor molecule in any zwitterionic product. Secondly, we wished to establish whether a range of donor molecules would all react to afford ylid type structures (Scheme 1).

Table 1
Analytical and physical data

Compound	Colour	Yield (%)	ν_{max}(CO)[b](cm^{-1})	Anal. (%)[a]	
				C	H
$[Ru(CO)_2(MeC{\equiv}CPh)(\eta^5\text{-}7,8\text{-}C_2B_9H_{11})]$ (**3c**)	Yellow	64	2070 s, 2024 s	38.2 (38.5)	4.7 (4.7)
$[Ru\{C(Me){=}C(Ph)PEt_3\}(CO)_2(\eta^5\text{-}7,8\text{-}C_2B_9H_{11})]$ (**4b**)	Yellow	90	2018 s, 1960 s	43.4 (43.6)	6.9 (6.5)
$[Ru\{C(Me){=}C(Ph)P(Ph)_2CH_2PPh_2\}(CO)_2(\eta^5\text{-}7,8\text{-}C_2B_9H_{11})]$ (**4c**)	Yellow	91	2019 s, 1961 s	58.1 (57.8)	5.4 (5.2)
$[Ru(CO)_2(AsPh_3)(\eta^5\text{-}7,8\text{-}C_2B_9H_{11})]$ (**5a**)	White	89	2052 s, 2004 s	44.7 (44.4)	4.4 (4.4)
$[Ru(CO)_2(SbPh_3)(\eta^5\text{-}7,8\text{-}C_2B_9H_{11})]$ (**5b**)	Pale yellow	90	2044 s, 1996 s	41.5 (41.1)	4.1 (4.1)
$[Ru(CO)_2\{Ph_2P(S)CH_2P(S)Ph_2\}(\eta^5\text{-}7,8\text{-}C_2B_9H_{11})_2]$ (**5c**)	Yellow	60	2046 s, 1994 s	49.5 (48.9)[c]	4.6 (5.1)
$[Ru_2(\mu\text{-}Ph_2PCH_2PPh_2)(CO)_4(\eta^5\text{-}7,8\text{-}C_2B_9H_{11})2]$ (**6**)	Yellow	45[d]	2050 s, 2002 s	40.5 (41.1)	4.2 (4.6)

[a] Calculated values are given in parentheses. [b] Measured in CH_2Cl_2. All complexes show a broad medium intensity band at ca. 2550 cm^{-1} due to cage B–H absorptions. [c] Crystallised with 0.5 molecule of pentane. [d] Yield when synthesised from **4c** and $Ph_2PCH_2PPh_2$: 35%.

Table 2
^{1}H-, ^{13}C-, ^{11}B- and ^{31}P-NMR data[a]

Compound	^{1}H (δ)[b]	^{13}C (δ)[c]	^{11}B (δ)[d]	^{31}P (δ)[e]
3c	2.71 (s, 2 H, cage CH), 2.76 (s, 3 H, Me), 7.53–7.44 (m, 5 H, Ph)	195.4 (CO), 132.3–122.9 (Ph), 74.2, 70.1 (C=C), 54.2 (cage CH), 11.9 (Me)	5.6 (1 B), −4.7 (3 B), −8.0 (2 B), −16.7 (1 B), −18.6 (2 B)	
4b	1.16 [d of t, 9 H, CH_2*Me*, J(PH) = 18, J(HH) = 8], 1.95 [d of q of q, 6 H, C*H*$_2$Me, J(PH) = 15, J(HH) = 8, J(HH) = 3], 2.18 (s, 2 H, cage CH), 3.05 [d of t, 3 H, Me, J(PH) = 9, J(HH) = 3], 7.02–7.38 (m, 5 H, Ph)	199.0 (CO), 141.8 [d, *C*Me, J(PC) = 17], 132.2–128.3 (Ph), 115.2 [d, CPh, J(PC) = 50], 41.2 (cage CH), 39.5 [d, C*Me*, J(PC) = 16], 16.3 [d, *C*H$_2$Me, J(PC) = 48], 6.7 [d, CH$_2$*Me*, J(PC) = 4]	−3.3 (1 B), −6.4 (1 B), −9.3 (2 B), −11.7 (2 B), −21.2 (3 B)	19.7 (s)
4c	2.22 (s, 2 H, cage CH), 2.54 [d, 3 H, Me, J(PH) = 3], 2.82 [d, 2 H, CH$_2$, J(PH) = 13], 6.93–7.80 (m, 25 H, Ph)	199.0 (CO), 142.0 [d, *C*Me, J(PC) = 20], 136.2–128.6 (Ph), 122.6 [d, CPh, J(PC) = 77], 43.0 [d, C*Me*, J(PC) = 18], 41.6 (cage CH), 28.9 [d of d, CH$_2$, J(PC) = 54 and 54]	−3.1 (1 B), −6.4 (1 B), −9.2 (2 B), −11.9 (2 B), −21.1 (3 B)	4.3 [d, J(PP) = 60], −30.4 [d, J(PP) = 60]
5a	2.57 (s, 2 H, cage CH), 7.34–7.57 (m, 15 H, Ph)	195.9 (CO), 134.0–128.8 (Ph), 46.8 (cage CH)	4.7 (1 B), −4.4 (1 B), −6.4 (2 B), −9.2 (2 B), −19.4 (3 B)	
5b	3.21 (s, 2 H, cage CH), 7.50–7.58 (m, 15 H, Ph)	195.2 (CO), 136.5–129.0 (Ph), 44.0 (cage CH)	5.4 (1 B), −3.5 (1 B), −6.8 (2 B), −10.2 (2 B), −18.8 (2 B), −20.1 (1 B)	
5c	2.60 (s, 2 H, cage CH), 4.05 [d of d, 2 H, CH$_2$, J(PH) = 12 and 12], 7.34–7.81 (m, 20 H, Ph)	196.3 (CO), 135.0–129.2 (Ph), 49.3 (cage CH), 35.3 [d of d, CH$_2$, J(PC) = 42 and 42]	3.5 (1 B), −7.4 (5 B), −17.6 (1 B), −21.1 (2B)	45.1 [d, J(PP) = 11], 33.0 [d, J(PP) = 11]
6	2.19 (s, 4 H, cage CH), 4.31 [t, 2 H, CH$_2$, J(PH) = 14], 7.24–7.43 (m, 20 H, Ph)	196.0 (CO), 132.8–126.9 (Ph), 47.6 (cage CH), 35.1 [t, CH$_2$, J(PC) = 9]	4.7 (1 B), −3.4 (1 B), −6.1 (2 B), −9.2 (2 B), −18.6 (3 B)	41.8 (s)

[a] Chemical shifts (δ) in ppm, coupling constants (J) in Hz, measurements at ambient temperatures in CD_2Cl_2. [b] Resonances for terminal BH protons occur as broad unresolved signals in the range ca. −2 to 3 ppm. [c] ^{1}H decoupled, chemical shifts are positive to high frequency of $SiMe_4$. [d] ^{1}H decoupled, chemical shifts are positive to high frequency of $BF_3 \cdot OEt_2$ (external). [e] ^{1}H decoupled, chemical shifts are positive to high frequency of H_3PO_4 (external).

Table 3
Selected internuclear distances (Å) and angles (°) for [Ru(CO)$_2$(MeC≡CPh)(η^5-7,8-$C_2B_9H_{11}$)] (**3c**), with estimated standard deviations in parentheses

Internuclear distances (Å)							
Ru(1)–C(3)	1.897(2)	C(1)–B(7)	1.730(3)	B(6)–B(7)	1.759(3)	C(15)–C(16)	1.475(3)
Ru(1)–C(4)	1.899(2)	C(2)–B(8)	1.705(3)	B(6)–B(10)	1.778(3)	C(16)–C(17)	1.228(3)
Ru(1)–C(1)	2.242(2)	C(2)–B(3)	1.713(3)	B(6)–B(11)	1.781(3)	C(17)–C(18)	1.456(3)
Ru(1)–C(2)	2.248(2)	C(2)–B(7)	1.736(3)	B(7)–B(11)	1.767(3)	C(18)–C(19)	1.397(3)
Ru(1)–B(5)	2.262(2)	B(3)–B(9)	1.767(3)	B(7)–B(8)	1.771(3)	C(18)–C(23)	1.403(3)
Ru(1)–B(3)	2.281(2)	B(3)–B(8)	1.786(3)	B(8)–B(11)	1.778(3)	C(19)–C(20)	1.388(3)
Ru(1)–B(4)	2.282(2)	B(3)–B(4)	1.839(3)	B(8)–B(9)	1.784(4)	C(20)–C(21)	1.382(3)
Ru(1)–C(17)	2.302(2)	B(4)–B(10)	1.794(3)	B(9)–B(11)	1.786(3)	C(21)–C(22)	1.386(3)
Ru(1)–C(16)	2.308(2)	B(4)–B(9)	1.797(3)	B(9)–B(10)	1.789(3)	C(22)–C(23)	1.382(3)
C(1)–C(2)	1.625(3)	B(4)–B(5)	1.823(3)	B(10)–B(11)	1.785(3)		
C(1)–B(6)	1.707(3)	B(5)–B(10)	1.774(3)	C(3)–O(3)	1.135(3)		
C(1)–B(5)	1.715(3)	B(5)–B(6)	1.789(3)	C(4)–O(4)	1.138(3)		
Internuclear angles (°)							
C(3)–Ru(1)–C(4)	88.93(9)	C(1)–Ru(1)–B(3)	75.58(8)	C(2)–Ru(1)–C(17)	87.27(8)		
C(3)–Ru(1)–C(1)	158.14(8)	C(2)–Ru(1)–B(3)	44.44(8)	B(5)–Ru(1)–C(17)	142.33(8)		
C(4)–Ru(1)–C(1)	110.66(8)	B(5)–Ru(1)–B(3)	79.70(8)	B(3)–Ru(1)–C(17)	110.99(8)		
C(3)–Ru(1)–C(2)	117.41(8)	C(3)–Ru(1)–B(4)	90.93(8)	B(4)–Ru(1)–C(17)	158.44(8)		
C(4)–Ru(1)–C(2)	153.10(8)	C(4)–Ru(1)–B(4)	98.47(8)	C(3)–Ru(1)–C(16)	106.11(8)		
C(1)–Ru(1)–C(2)	42.45(7)	C(1)–Ru(1)–B(4)	77.04(8)	C(4)–Ru(1)–C(16)	82.00(8)		
C(3)–Ru(1)–B(5)	134.41(8)	C(2)–Ru(1)–B(4)	76.98(8)	C(1)–Ru(1)–C(16)	86.81(7)		
C(4)–Ru(1)–B(5)	81.84(8)	B(5)–Ru(1)–B(4)	47.30(8)	C(2)–Ru(1)–C(16)	94.83(7)		
C(1)–Ru(1)–B(5)	44.76(8)	B(3)–Ru(1)–B(4)	47.53(8)	B(5)–Ru(1)–C(16)	116.47(8)		
C(2)–Ru(1)–B(5)	75.69(8)	C(3)–Ru(1)–C(17)	83.26(8)	B(3)–Ru(1)–C(16)	133.45(8)		
C(3)–Ru(1)–B(3)	82.82(8)	C(4)–Ru(1)–C(17)	102.15(8)	B(4)–Ru(1)–C(16)	162.96(8)		
C(4)–Ru(1)–B(3)	144.51(9)	C(1)–Ru(1)–C(17)	101.20(7)	C(17)–Ru(1)–C(16)	30.90(7)		
C(17)–C(16)–C(15)	161.6(2)	C(16)–C(17)–C(18)	156.6(2)	O(3)–C(3)–Ru(1)	175.9(2)		
O(4)–C(4)–Ru(1)	175.9(2)						

2. Results and discussion

The complex **3c** was readily obtained by adding the alkyne MeC≡CPh to a CH_2Cl_2 solution of **2** prepared in situ from [NEt_4][RuI(CO)$_2$(η^5-7,8-$C_2B_9H_{11}$)] and $AgBF_4$ in THF. As previously reported ([1]a), the replacement of THF solvent by CH_2Cl_2 in this latter preparation results in the generation of a mixture in which **2**, the 16-electron species [Ru(CO)$_2$(η^5-7,8-$C_2B_9H_{11}$)] and free THF are present. The mixture is a ready source of the Ru(CO)$_2$(η^5-7,8-$C_2B_9H_{11}$) fragment. Data characterising **3c** are given in Tables 1 and 2. A single-crystal X-ray diffraction study was carried out in order to place the molecular structures of the alkyne complexes of type **3** on a firm basis and also to use the X-ray generated atomic co-ordinates for semi-empirical molecular orbital calculations which will be discussed later. Selected parameters are listed in Table 3 and the molecule is shown in Fig. 1.

The ruthenium atom is pentahapto co-ordinated on one side by the *nido*-7,8-C_2B_9 fragment in the usual manner. The connectivities between the metal and the cage atoms [Ru(1)–C(1) = 2.242(2), Ru(1)–C(2) = 2.248(2), Ru(1)–B(3) = 2.281(2), Ru(1)–B(4) = 2.282(2), Ru(1)–B(5) = 2.262(2) Å] are similar to those observed in other molecules with the *closo*-3,1,2-RuC_2B_9 framework ([1]a,b). On the other side, the metal is ligated by two CO groups in an essentially linear manner [Ru–C–O$_{av.}$ = 175.9(2) °] and by the MeC≡CPh molecule [Ru(1)–C(16) = 2.308(2), Ru(1)–C(17) = 2.302(2) Å]. The C(16)–C(17) separation [1.228(3) Å] is perceptibly shorter than the mean value (1.269 Å) found in alkyne–metal complexes [2]. The ligated alkyne C≡C–C bond angles [C(17)–C(16)–C(15) = 161.6(2), C(16)–C(17)–C(18) = 156.6(2) °] are, however, comparable with those found in other transition metal–alkyne complexes [3].

The NMR data (Table 2) for **3c** are in accord with the structure determined by X-ray diffraction. The ^{1}H-NMR spectrum shows diagnostic peaks of relative intensity 2:3 at δ 2.71 and 2.76, respectively, for the cage CH and alkyne Me groups. The ^{13}C{^{1}H}-NMR spectrum displayed a resonance for the cage CH groups at δ 54.2 and peaks for the ligated carbons of the alkyne at δ 70.1 and 74.2. The observation of only one signal for the CO ligands at δ 195.4 must be due to rotation of the η^2-MeC≡CPh group about an axis through the Ru atom and the mid-point of the C≡C bond, thus demonstrating an apparent equivalence of the carbonyls on the NMR time scale. Treatment of **3c** in CH_2Cl_2 with PEt_3 gave the ylid compound [Ru{C(Me)=C(Ph)PEt_3}(CO)$_2$(η^5-7,8-$C_2B_9H_{11}$)] (**4b**) the structure of which was established by an X-ray diffraction study. The results are given in Table 4 and the molecule is shown in Fig. 2.

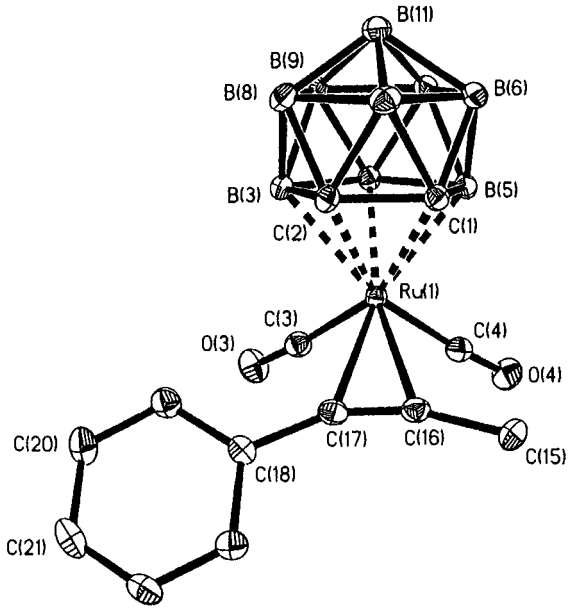

Fig. 1. Molecular structure of $[Ru(CO)_2(MeC{\equiv}CPh)(\eta^5\text{-}7,8\text{-}C_2B_9H_{11})]$ (**3c**) showing the atom labelling scheme. Hydrogen atoms are omitted for clarity. Thermal ellipsoids are shown at the 40% probability level.

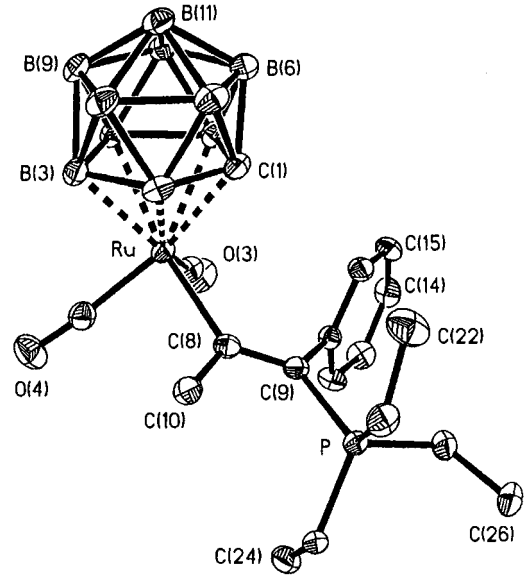

Fig. 2. Molecular structure of $[Ru\{C(Me){=}C(Ph)PEt_3\}(CO)_2(\eta^5\text{-}7,8\text{-}C_2B_9H_{11})]$ (**4b**) showing the atom labelling scheme. Hydrogen atoms are omitted for clarity. Thermal ellipsoids are shown at the 40% probability level.

The ruthenium atom is co-ordinated by the *nido*-$C_2B_9H_{11}$ cage and two CO molecules in the usual manner. Interest focuses on the attachment of the PEt_3 group which has attacked the alkyne in the precursor **3c** in such a manner that in **4b** it is bonded to the carbon atom C(9) carrying the Ph group [P–C(9) = 1.820(2) Å]. The Me and Ph groups are *transoid* to one another and the C(8)–C(9) separation [1.344(3) Å] corresponds

Table 4
Selected internuclear distances (Å) and angles (°) for $[Ru(CO)_2\{C(Me){=}C(Ph)PEt_3\}(\eta^5\text{-}7,8\text{-}C_2B_9H_{11})]$ (**4b**), with estimated standard deviations in parentheses

Internuclear distances (Å)							
Ru–C(3)	1.859(2)	Ru–C(4)	1.870(2)	Ru–C(8)	2.141(2)	Ru–C(2)	2.253(2)
Ru–C(1)	2.259(2)	Ru–B(3)	2.281(3)	Ru–B(5)	2.307(2)	Ru–B(4)	2.343(2)
P–C(23)	1.811(2)	P–C(25)	1.812(2)	P–C(21)	1.815(2)	P–C(9)	1.820(2)
C(1)–C(2)	1.615(3)	C(1)–B(5)	1.694(3)	C(1)–B(6)	1.699(3)	C(1)–B(7)	1.730(3)
C(2)–B(8)	1.696(3)	C(2)–B(3)	1.719(3)	C(2)–B(7)	1.728(4)	B(3)–B(9)	1.772(4)
B(3)–B(8)	1.797(4)	B(3)–B(4)	1.799(4)	B(4)–B(9)	1.783(4)	B(4)–B(10)	1.786(4)
B(4)–B(5)	1.815(3)	B(5)–B(10)	1.778(4)	B(5)–B(6)	1.784(4)	B(6)–B(7)	1.765(4)
B(6)–B(11)	1.768(4)	B(6)–B(10)	1.772(4)	B(7)–B(8)	1.761(4)	B(7)–B(11)	1.763(4)
B(8)–B(9)	1.768(4)	B(8)–B(11)	1.782(4)	B(9)–B(11)	1.773(4)	B(9)–B(10)	1.777(4)
B(10)–B(11)	1.776(4)	C(3)–O(3)	1.144(3)	C(4)–O(4)	1.144(3)	C(8)–C(9)	1.344(3)
C(8)–C(10)	1.520(3)	C(9)–C(11)	1.506(3)				
Internuclear angles (°)							
C(3)–Ru–C(4)	88.21(11)	C(3)–Ru–C(8)	94.60(9)	C(4)–Ru–C(8)	88.42(9)		
C(3)–Ru–C(2)	159.15(10)	C(4)–Ru–C(2)	111.88(10)	C(8)–Ru–C(2)	91.60(8)		
C(3)–Ru–C(1)	118.02(9)	C(4)–Ru–C(1)	153.75(10)	C(8)–Ru–C(1)	90.32(8)		
C(2)–Ru–C(1)	41.94(8)	C(3)–Ru–B(3)	137.06(10)	C(4)–Ru–B(3)	85.62(10)		
C(8)–Ru–B(3)	127.58(9)	C(2)–Ru–B(3)	44.56(9)	C(1)–Ru–B(3)	74.48(9)		
C(3)–Ru–B(5)	85.88(10)	C(4)–Ru–B(5)	147.90(9)	C(8)–Ru–B(5)	123.48(8)		
C(2)–Ru–B(5)	74.15(9)	C(1)–Ru–B(5)	43.53(8)	B(3)–Ru–B(5)	77.59(9)		
C(3)–Ru–B(4)	95.33(10)	C(4)–Ru–B(4)	103.53(9)	C(8)–Ru–B(4)	164.67(9)		
C(2)–Ru–B(4)	75.17(9)	C(1)–Ru–B(4)	74.70(8)	B(3)–Ru–B(4)	45.75(9)		
B(5)–Ru–B(4)	45.93(8)	C(23)–P–C(25)	106.84(11)	C(23)–P–C(21)	107.97(11)		
C(25)–P–C(21)	106.39(12)	C(23)–P–C(9)	114.96(10)	C(25)–P–C(9)	108.14(10)		
C(21)–P–C(9)	112.08(11)	O(3)–C(3)–Ru	173.5(2)	O(4)–C(4)–Ru	176.8(2)		
C(9)–C(8)–C(10)	120.2(2)	C(9)–C(8)–Ru	126.5(2)	C(10)–C(8)–Ru	113.19(14)		
C(8)–C(9)–C(11)	125.4(2)	C(8)–C(9)–P	121.1(2)	C(11)–C(9)–P	113.4(2)		

precisely to the mean value found in numerous complexes where a metal carries an η^1-C(R^1)=C(R^2)R^3 group [2]. The Ru–C(8) separation [2.141(2) Å] may be compared with the Ru–C(CF_3) σ-bond distance [2.082(5) Å] in [Ru{σ,η^2-C(CF_3)=C(CF_3)C(CF_3)=C(CF_3)H}(PPh_3)(η^5-C_5H_5)] [4].

The various resonances seen in the NMR spectra of **4b** (Table 2) are as expected for the structure established by the X-ray diffraction study. It is interesting that there was no evidence in the spectra for peaks attributable to an isomer of **4b** with the PEt_3 moiety attached to the CMe group, viz. [Ru{C(Ph)=C(Me)PEt_3}$(CO)_2$(η^5-7,8-$C_2B_9H_{11}$)]. Evidently the formation of **4b** is regiospecific, a feature discussed further below.

The reaction between **3c** and $Ph_2PCH_2PPh_2$ was next investigated. If these reagents are mixed in 1:1 mol ratio the product obtained is [Ru{C(Me)=C(Ph)P(Ph)$_2$ CH_2PPh_2}$(CO)_2$(η^5-7,8-$C_2B_9H_{11}$)] (**4c**) characterised by the data in Tables 1 and 2. Again the structure is one of the ylid type, formulated with the $Ph_2PCH_2PPh_2$ molecule bonded through phosphorus to the CPh moiety of the Ru–C(Me)=C(Ph) group. This is in accord with similarities in the $^{13}C\{^1H\}$-NMR spectrum for the signal for the *C*Me nucleus in **4c** [δ 142.0, J(PC) = 20 Hz] with that in **4b** [δ 141.8, J(PC) = 17 Hz]. Furthermore, a partial X-ray structure analysis on a single-crystal of **4c** clearly revealed that the co-ordinated phosphorus atom of the $Ph_2PCH_2PPh_2$ molecule is bound to the CPh group to give an η^1-C(Me)=C(Ph)P(Ph)$_2$$CH_2PPh_2$ ligand with the methyl and phenyl groups lying *transoid* to one another as in **4b**. Unfortunately the structure analysis could not be completed due to severe disorder of the free end of the $Ph_2PCH_2PPh_2$ molecule. The $^{31}P\{^1H\}$-NMR spectrum of **4c** shows two resonances as expected. That at δ −30.4 is diagnostic for the phosphorus nucleus of the free PPh_2 group which is not attached to the =C(Ph) moiety [5], hence the resonance at δ 4.3 must be assigned to the =C(Ph)*P*Ph_2 nucleus. Careful examination of the NMR spectra of **4c** revealed the absence of any signals due to the presence of another isomer, as was observed with **4b**.

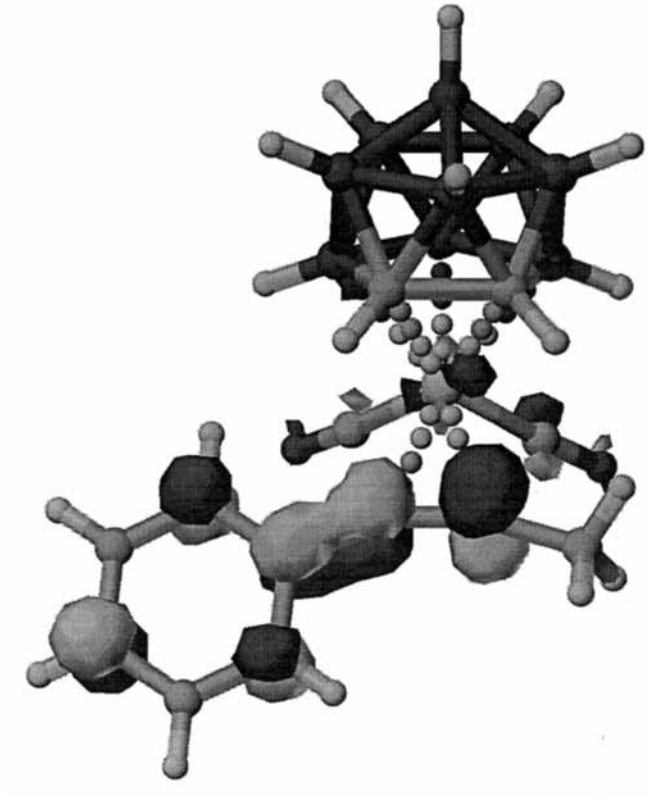

Fig. 3. ZINDO calculation of the LUMO of **3c**.

Following the successful characterisation of the phosphine adducts **4b** and **4c**, a semi-empirical ZINDO molecular orbital calculation was carried out on the alkyne complex **3c** to gain further insight into the nature of these phosphine addition reactions [6]. The results of this calculation reveal that the LUMO (Fig. 3) in **3c** is primarily localised on the alkyne and it is therefore sensible that nucleophilic addition of phosphines is experimentally observed to occur at the alkyne rather than at the metal centre. The ligated carbon atoms of the alkyne have substantial π^* antibonding character but the LUMO is also delocalised over the adjacent phenyl substituent and there is a net π bonding contribution to the alkyne C–Ph bond. As a result the LUMO tends to be localised in the region of the C–Ph bond which is consistent with the experimental observation that nucleophilic addition of phosphines occurs regiospecifically at the alkyne CPh carbon centre. Similar calculations were also carried out using both Extended Hückel and Iterative Extended Hückel methods to test the sensitivity of the results to the computational method and parameterisation. The computed LUMO was similar in all cases but there was some variation in the extent of the metal contribution to the low lying LUMO orbitals. For this reason we cannot rule out the possibility that initial attack of phosphine might occur at the metal followed by regiospecific transfer to the alkyne CPh carbon centre. However, this mode of nucleophilic attack would likely yield an alkenyl ligand with the methyl and phenyl groups lying *cisoid* to one another. Previous studies on cationic alkyne complexes of the type [PtMe(L)$_2$(RC≡CR)][PF_6] (L = phosphine or arsine, R = alkyl or aryl) and [Fe(CO)(L)(MeC≡CPh)(η^5-C_5H_5)][BF_4] [L = PPh_3, P$(OPh)_3$] have established a *trans*-attack mechanism for nucleophiles without prior co-ordination to the metal centre [7].

Table 5
Selected internuclear distances (Å) and angles (°) for $[Ru_2(\mu\text{-}Ph_2PCH_2PPh_2)(CO)_4(\eta^5\text{-}7,8\text{-}C_2B_9H_{11})_2]$ (**6**), with estimated standard deviations in parentheses

Internuclear distances (Å)							
Ru(1)–C(2)	1.880(7)	Ru(1)–C(1)	1.886(7)	Ru(1)–C(11)	2.234(7)	Ru(1)–C(12)	2.240(6)
Ru(1)–B(15)	2.266(8)	Ru(1)–B(13)	2.286(7)	Ru(1)–B(14)	2.303(7)	Ru(1)–P(1)	2.377(2)
C(1)–O(1)	1.143(8)	C(2)–O(2)	1.141(7)	Ru(2)–C(3)	1.884(6)	Ru(2)–C(4)	1.889(7)
Ru(2)–C(22)	2.245(6)	Ru(2)–C(21)	2.253(6)	Ru(2)–B(23)	2.283(7)	Ru(2)–B(25)	2.290(7)
Ru(2)–B(24)	2.323(7)	Ru(2)–P(2)	2.364(2)	C(3)–O(3)	1.138(7)	C(4)–O(4)	1.142(7)
P(1)–C(41)	1.819(6)	P(1)–C(31)	1.821(6)	P(1)–C(5)	1.855(5)	C(5)–P(2)	1.859(5)
P(2)–C(61)	1.818(6)	P(2)–C(51)	1.820(6)				
Internuclear angles (°)							
C(2)–Ru(1)–C(1)	89.7(3)	C(2)–Ru(1)–C(11)	159.2(3)	C(1)–Ru(1)–C(11)	109.7(3)		
C(2)–Ru(1)–C(12)	118.1(3)	C(1)–Ru(1)–C(12)	152.1(3)	C(11)–Ru(1)–C(12)	42.4(3)		
C(2)–Ru(1)–B(15)	135.3(3)	C(1)–Ru(1)–B(15)	82.9(3)	C(11)–Ru(1)–B(15)	44.8(3)		
C(12)–Ru(1)–B(15)	75.5(3)	C(2)–Ru(1)–B(13)	84.9(3)	C(1)–Ru(1)–B(13)	147.0(3)		
C(11)–Ru(1)–B(13)	74.7(3)	C(12)–Ru(1)–B(13)	44.0(3)	B(15)–Ru(1)–B(13)	78.4(3)		
C(2)–Ru(1)–B(14)	93.7(3)	C(1)–Ru(1)–B(14)	101.8(3)	C(11)–Ru(1)–B(14)	75.4(3)		
C(12)–Ru(1)–B(14)	75.4(3)	B(15)–Ru(1)–B(14)	46.0(3)	B(13)–Ru(1)–B(14)	46.4(3)		
C(2)–Ru(1)–P(1)	88.4(2)	C(1)–Ru(1)–P(1)	91.5(2)	C(11)–Ru(1)–P(1)	98.2(2)		
C(12)–Ru(1)–P(1)	91.8(2)	B(15)–Ru(1)–P(1)	135.6(2)	B(13)–Ru(1)–P(1)	120.7(2)		
B(14)–Ru(1)–P(1)	166.5(2)	O(1)–C(1)–Ru(1)	177.5(6)	O(2)–C(2)–Ru(1)	177.9(5)		
C(3)–Ru(2)–C(4)	91.5(3)	C(3)–Ru(2)–C(22)	116.3(2)	C(4)–Ru(2)–C(22)	152.2(2)		
C(3)–Ru(2)–C(21)	158.0(2)	C(4)–Ru(2)–C(21)	109.8(2)	C(22)–Ru(2)–C(21)	42.5(2)		
C(3)–Ru(2)–B(23)	83.5(3)	C(4)–Ru(2)–B(23)	147.9(3)	C(22)–Ru(2)–B(23)	44.6(2)		
C(21)–Ru(2)–B(23)	75.5(2)	C(3)–Ru(2)–B(25)	137.7(3)	C(4)–Ru(2)–B(25)	84.2(3)		
C(22)–Ru(2)–B(25)	74.9(2)	C(21)–Ru(2)–B(25)	44.2(2)	B(23)–Ru(2)–B(25)	78.6(3)		
C(3)–Ru(2)–B(24)	94.5(2)	C(4)–Ru(2)–B(24)	102.1(3)	C(22)–Ru(2)–B(24)	76.5(2)		
C(21)–Ru(2)–B(24)	76.2(2)	B(23)–Ru(2)–B(24)	47.2(3)	B(25)–Ru(2)–B(24)	46.2(2)		
C(3)–Ru(2)–P(2)	89.2(2)	C(4)–Ru(2)–P(2)	89.6(2)	C(22)–Ru(2)–P(2)	91.3(2)		
C(21)–Ru(2)–P(2)	96.1(2)	B(23)–Ru(2)–P(2)	121.9(2)	B(25)–Ru(2)–P(2)	132.7(2)		
B(24)–Ru(2)–P(2)	167.6(2)	O(3)–C(3)–Ru(2)	176.8(5)	O(4)–C(4)–Ru(2)	178.2(5)		
C(41)–P(1)–C(31)	108.4(3)	C(41)–P(1)–C(5)	106.8(2)	C(31)–P(1)–C(5)	108.0(3)		
C(41)–P(1)–Ru(1)	114.7(2)	C(31)–P(1)–Ru(1)	109.2(2)	C(5)–P(1)–Ru(1)	109.6(2)		
P(1)–C(5)–P(2)	128.6(3)	C(61)–P(2)–C(51)	108.4(3)	C(61)–P(2)–C(5)	104.8(2)		
C(51)–P(2)–C(5)	107.2(2)	C(61)–P(2)–Ru(2)	114.5(2)	C(51)–P(2)–Ru(2)	109.8(2)		
C(5)–P(2)–Ru(2)	111.8(2)						

In contrast with the formation of the ylid complexes **4b** and **4c**, treatment of **3c** with the donor molecules $AsPh_3$ or $SbPh_3$ resulted in displacement of the alkyne ligand from the latter and formation of the complexes $[Ru(CO)_2(L)(\eta^5\text{-}7,8\text{-}C_2B_9H_{11})]$ (**5a**, L = $AsPh_3$; **5b**, L = $SbPh_3$). Data characterising these species are given in Tables 1 and 2. The reaction between **3c** and $Ph_2P(S)CH_2P(S)Ph_2$ in 1:1 mol ratio followed a similar path to form $[Ru(CO)_2\{Ph_2P(S)CH_2P(S)Ph_2\}(\eta^5\text{-}7,8\text{-}C_2B_9H_{11})]$ (**5c**) rather than an ylid complex. The IR and

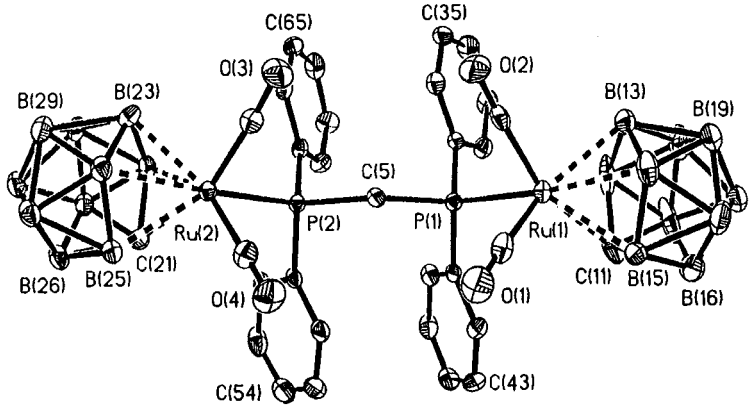

Fig. 4. Molecular structure of $[Ru_2(\mu\text{-}Ph_2PCH_2PPh_2)(CO)_4(\eta^5\text{-}7,8\text{-}C_2B_9H_{11})_2]$ (**6**) showing the atom labelling scheme. Hydrogen atoms are omitted for clarity. Thermal ellipsoids are shown at the 40% probability level.

Table 6
Data for X-ray crystal structure analyses

	3c	4b	6
Crystal dimensions (mm)	$0.40 \times 0.64 \times 0.78$	$0.50 \times 0.50 \times 0.15$	$0.25 \times 0.20 \times 0.05$
Formula	$C_{13}H_{19}B_9O_2Ru$	$C_{19}H_{34}B_9O_2PRu$	$C_{35}H_{46}B_{18}Cl_2O_4P_2Ru_2$
M_r	405.64	523.79	1060.28
Crystal colour, shape	Pale yellow	Pale yellow	Pale yellow
Crystal system	Monoclinic	Monoclinic	Monoclinic
Space group	$P2_1/n$	$P2_1/c$	$P2_1/n$
T (K)	173(2)	173(2)	173(2)
Crystal data			
a (Å)	16.257(4)	11.873(1)	13.670(2)
b (Å)	6.9867(12)	15.106(2)	22.845(2)
c (Å)	17.656(3)	15.086(3)	15.325(2)
β (°)	116.436(8)	110.33(1)	102.55(1)
V (Å^3)	1795.7(6)	2537.2(7)	4671.4(9)
Z	4	4	4
D_{calc} (g cm^{-3})	1.500	1.371	1.508
μ(Mo–K$_\alpha$) (cm^{-1})	8.74	6.96	8.67
F(000) (e)	808	1072	2120
Data frame collection time (s)	10	20	40
2θ range (°)	4.6–50.0	5.0–55.0	5.0–50.0
No. of reflections			
Measured	8159	15523	20768
Unique	3146	5799	7851
Observed	3144	5799	7851
Reflection limits			
h	−19 to 17	−9 to 15	−15 to 16
k	−8 to 7	−19 to 19	−26 to 22
l	−21 to 16	−19 to 15	−12 to 17
Final residuals	$wR_2 = 0.0527$[a] ($R_1 = 0.0199$)[b]	$wR_2 = 0.0648$[a] ($R_1 = 0.0276$)[b]	$wR_2 = 0.0984$[a] ($R_1 = 0.0530$)[b]
Weighting factors	$a = 0.0227$, $b = 1.5380$[a]	$a = 0.0363$, $b = 0.0000$[a]	$a = 0.0085$, $b = 27.21$[a]
Largest difference peak and hole (e Å^{-3})	0.25/−0.45	0.52/−0.68	1.61/−1.60
Goodness-of-fit	1.147	0.976	1.186

[a] Structure was refined on F_o^2 using all data: $wR_2 = [\Sigma\{w(F_o^2 - F_c^2)^2\}/\Sigma w(F_o^2)^2]^{1/2}$ where $w^{-1} = [\sigma^2(F_o^2) + (aP)^2 + bP]$ and $P = [\max(F_o^2, 0) + 2F_c^2]/3$.
[b] The value in parentheses is given for comparison with refinements based on F_o with a typical threshold of $F_o > 4\sigma(F_o)$ and $R_1 = \Sigma\|F_o| - |F_c\|/\Sigma|F_o|$ and $w^{-1} = [\sigma^2(F_o) + gF_o^2]$.

NMR data for complexes **5a–c** are in accord with their C_s structures (Tables 1 and 2). In particular, the simplicity of the $^{11}B\{^1H\}$-NMR spectra of these compounds (integrated signal ratios: **5a**, 1:1:2:2:3; **5b**, 1:1:2:2:2:1; **5c**, 1:5:1:2) reflects this symmetry.

Finally, an attempt was made to co-ordinate the unattached PPh_2 group in **4c** to the 16-electron fragment $Ru(CO)_2(\eta^5\text{-}7,8\text{-}C_2B_9H_{11})$ by treating the former with a CH_2Cl_2 solution obtained by adding $AgBF_4$ to $[NEt_4][RuI(CO)_2(\eta^5\text{-}7,8\text{-}C_2B_9H_{11})]$. The product of this reaction was, however, the diruthenium complex $[Ru_2(\mu\text{-}Ph_2PCH_2PPh_2)(CO)_4(\eta^5\text{-}7,8\text{-}C_2B_9H_{11})_2]$ (**6**), data for which are given in Tables 1 and 2. Evidently the reaction proceeds with loss of the MeC≡CPh group possibly from an intermediate $[Ru_2(\mu\text{-}C(Me)=C(Ph)P(Ph)_2CH_2PPh_2)(CO)_4(\eta^5\text{-}7,8\text{-}C_2B_9H_{11})_2]$. Not surprisingly **6** is readily synthesised in a more rational manner by treating **2** with $Ph_2PCH_2PPh_2$ in a 2:1 mol ratio. The nature of **6** was firmly established by an X-ray diffraction study. Selected structural parameters are given in Table 5 and the molecule is shown in Fig. 4.

The two $Ru(CO)_2(\eta^5\text{-}7,8\text{-}C_2B_9H_{11})$ fragments are bridged by the $Ph_2PCH_2PPh_2$ ligand with the Ru–P separations (av. 2.371 Å) being very similar to those observed for such distances in other ruthenacarborane complexes ([1]b), [8]. The four CO molecules are essentially linearly bound to their respective metal centres [Ru–C–O$_{av.}$ = 177.6 °] and each cage is pentahapto co-ordinated to its respective ruthenium atom.

The IR spectrum of **6** shows two ν_{max}(CO) bands at 2050 and 2002 cm^{-1}. The NMR spectra reflect its C_s symmetry in solution with resonances for the cage CH nuclei at δ 2.19 in the ^{1}H-NMR spectrum and at δ 47.6 in the $^{13}C\{^1H\}$-NMR spectrum (Table 2). The latter accordingly reveals a single resonance for all four CO carbon nuclei at δ 196.0. The $^{11}B\{^1H\}$-NMR spectrum is also relatively simple with five signals in the ratio 1:1:2:2:3. As far as we are aware **6** is the first molecule to be described where two metallaborane groups are bridged by a $Ph_2PCH_2PPh_2$ ligand.

Table 7
Atomic positional parameters (fractional co-ordinates $\times 10^4$) and equivalent isotropic displacement parameters ($Å^2 \times 10^3$) for **3c**

Atom	x	y	z	U(eq)[a]
Ru(1)	4256(1)	5903(1)	1806(1)	15(1)
C(1)	2973(1)	4784(3)	1826(1)	19(1)
C(2)	3185(1)	3669(3)	1123(1)	20(1)
B(3)	3306(2)	5212(3)	426(1)	20(1)
B(4)	3124(2)	7608(3)	755(1)	20(1)
B(5)	2930(2)	7216(3)	1684(1)	19(1)
B(6)	1910(2)	5815(3)	1375(2)	22(1)
B(7)	2081(2)	3543(4)	1039(2)	24(1)
B(8)	2284(2)	3839(4)	140(2)	25(1)
B(9)	2222(2)	6334(4)	−94(1)	23(1)
B(10)	1986(2)	7561(3)	676(1)	22(1)
B(11)	1464(2)	5298(4)	276(2)	25(1)
C(3)	5094(1)	6505(3)	1362(1)	24(1)
O(3)	5551(1)	6877(2)	1050(1)	35(1)
C(4)	4771(1)	7912(3)	2603(1)	23(1)
O(4)	5030(1)	9165(2)	3062(1)	34(1)
C(15)	5028(2)	4305(3)	3803(1)	30(1)
C(16)	5059(1)	4041(3)	2988(1)	22(1)
C(17)	5263(1)	3426(3)	2442(1)	21(1)
C(18)	5775(1)	2302(3)	2101(1)	21(1)
C(19)	5544(2)	2196(3)	1239(1)	26(1)
C(20)	6111(2)	1215(3)	972(2)	32(1)
C(21)	6897(2)	316(3)	1552(2)	33(1)
C(22)	7110(2)	350(3)	2405(2)	30(1)
C(23)	6557(1)	1331(3)	2682(1)	24(1)

[a] Equivalent isotropic U defined as one-third of the trace of the orthogonalised U_{ij} tensor.

3. Conclusion

Further work with complex **3c** and analogues thereof may be warranted in light of the curious ejection of the alkyne molecule in certain reactions. The chemistry of this species may be expanded by studying its reactivity with a range of nucleophilic organic or transition metal–ligand fragments.

4. Experimental section

4.1. General procedures

All experiments were conducted under an atmosphere of dry nitrogen or argon using Schlenk-line techniques. Solvents were freshly distilled under nitrogen from appropriate drying agents before use. Chromatography columns (ca. 30 cm in length and 3 cm in diameter) were packed under nitrogen with silica gel (Acros, 60–200 mesh). The NMR spectra were recorded at ambient temperatures in CD_2Cl_2, at the following frequencies: ^1H at 360.1, ^{13}C at 90.6, ^{31}P at 145.8 and ^{11}B at 115.3 MHz. IR spectra were measured with a Bruker IFS 25 spectrometer. The compound $[NEt_4][RuI(CO)_2(\eta^5\text{-}7,8\text{-}C_2B_9H_{11})]$ was obtained as previously described ([1]a). The reagent $Ph_2P(S)CH_2P(S)Ph_2$ was prepared according to the literature method [9].

4.2. Synthesis of $[Ru(CO)_2(MeC{\equiv}CPh)(\eta^5\text{-}7,8\text{-}C_2B_9H_{11})]$

The compound $[NEt_4][RuI(CO)_2(\eta^5\text{-}7,8\text{-}C_2B_9H_{11})]$ (0.21 g, 0.38 mmol) in THF (15 cm^3) was treated with $AgBF_4$ (0.08 g, 0.41 mmol). After removal of solvent in vacuo, the residue was taken up in CH_2Cl_2 (15 cm^3), cooled to ca. −95°C with a toluene–liquid nitrogen bath and treated with an excess of MeC≡CPh (0.22 cm^3, 1.92 mmol). The reaction mixture was warmed slowly to room temperature (r.t.). Monitoring of changes in the IR spectrum in the ν_{max}(CO) region revealed that the reaction was complete in ca. 60 min. After filtration through a Celite pad to remove AgI, the yellow filtrate containing the product was evaporated in vacuo and the residue obtained crystallised from CH_2Cl_2–*n*-pentane (1:2, 5 cm^3) to yield pale yellow crystals of $[Ru(CO)_2(MeC{\equiv}CPh)(\eta^5\text{-}7,8\text{-}C_2B_9H_{11})]$ (**3c**) (0.10 g).

Table 8
Atomic positional parameters (fractional co-ordinates $\times 10^4$) and equivalent isotropic displacement parameters ($Å^2 \times 10^3$) for **4b**

Atom	x	y	z	U(eq)[a]
Ru	9313(1)	2158(1)	1835(1)	23(1)
P	13429(1)	2063(1)	3958(1)	24(1)
C(1)	9039(2)	1072(2)	2770(2)	27(1)
C(2)	8560(2)	2012(2)	3007(2)	29(1)
B(3)	7522(2)	2466(2)	2013(2)	28(1)
B(4)	7335(2)	1671(2)	1085(2)	26(1)
B(5)	8393(2)	790(2)	1617(2)	26(1)
B(6)	7953(2)	283(2)	2515(2)	31(1)
B(7)	8087(2)	1064(2)	3416(2)	34(1)
B(8)	7099(2)	1946(2)	2922(2)	34(1)
B(9)	6318(2)	1700(2)	1719(2)	31(1)
B(10)	6846(2)	666(2)	1459(2)	30(1)
B(11)	6665(2)	836(2)	2567(2)	33(1)
C(3)	9841(2)	1839(2)	855(2)	33(1)
O(3)	10054(2)	1646(1)	197(1)	50(1)
C(4)	9273(2)	3333(2)	1437(2)	33(1)
O(4)	9192(2)	4049(1)	1173(1)	48(1)
C(8)	11079(2)	2398(1)	2826(2)	25(1)
C(9)	12067(2)	1914(1)	2936(2)	24(1)
C(10)	11128(2)	3166(2)	3490(2)	29(1)
C(11)	12172(2)	1197(1)	2274(2)	25(1)
C(12)	12860(2)	1338(2)	1706(2)	32(1)
C(13)	13008(2)	688(2)	1108(2)	35(1)
C(14)	12456(2)	−118(2)	1061(2)	36(1)
C(15)	11778(2)	−280(2)	1619(2)	35(1)
C(16)	11642(2)	364(1)	2228(2)	29(1)
C(21)	13159(2)	1926(2)	5063(2)	35(1)
C(22)	12366(3)	1142(2)	5079(2)	52(1)
C(23)	14182(2)	3114(1)	4002(2)	33(1)
C(24)	14340(2)	3379(2)	3082(2)	39(1)
C(25)	14486(2)	1206(2)	3933(2)	34(1)
C(26)	15616(2)	1162(2)	4824(2)	44(1)

[a] Equivalent isotropic U defined as one-third of the trace of the orthogonalised U_{ij} tensor.

Table 9
Atomic positional parameters (fractional co-ordinates $\times 10^4$) and equivalent isotropic displacement parameters ($Å^2 \times 10^3$) for **6**

Atom	x	y	z	U(eq)[a]
Ru(1)	11183(1)	−785(1)	7057(1)	22(1)
C(11)	11935(6)	−1650(3)	7379(6)	54(2)
C(12)	11374(5)	−1615(3)	6335(6)	54(2)
B(13)	11767(6)	−1033(4)	5818(5)	42(2)
B(14)	12708(5)	−682(4)	6666(6)	41(2)
B(15)	12763(6)	−1083(4)	7674(5)	42(2)
B(16)	13172(8)	−1800(4)	7497(6)	59(3)
B(17)	12269(8)	−2153(4)	6673(8)	72(4)
B(18)	12179(6)	−1760(4)	5666(6)	51(2)
B(19)	13054(6)	−1176(4)	5886(6)	41(2)
B(110)	13665(6)	−1217(4)	7014(6)	51(2)
B(111)	13349(6)	−1867(4)	6399(6)	45(2)
C(1)	11364(5)	−325(3)	8102(5)	34(2)
O(1)	11508(4)	−41(2)	8731(4)	53(1)
C(2)	10613(4)	−137(3)	6375(4)	29(1)
O(2)	10294(4)	258(2)	5952(3)	44(1)
Ru(2)	7192(1)	586(1)	8107(1)	19(1)
C(21)	5964(4)	326(3)	8799(4)	25(1)
C(22)	5547(4)	386(3)	7723(4)	25(1)
B(23)	5803(6)	1061(3)	7331(5)	33(2)
B(24)	6440(6)	1469(3)	8331(5)	29(2)
B(25)	6536(5)	957(3)	9245(5)	28(2)
B(26)	5296(5)	766(3)	9350(5)	30(2)
B(27)	4678(5)	387(3)	8388(5)	28(2)
B(28)	4577(5)	868(3)	7466(5)	32(2)
B(29)	5113(5)	1551(3)	7867(5)	33(2)
B(210)	5560(6)	1484(3)	9047(5)	32(2)
B(211)	4419(6)	1133(3)	8505(5)	33(2)
C(3)	7782(4)	877(3)	7191(4)	27(1)
O(3)	8096(4)	1063(2)	6620(3)	44(1)
C(4)	8425(5)	632(3)	8948(4)	32(2)
O(4)	9162(4)	673(2)	9465(3)	50(1)
P(1)	9546(1)	−1061(1)	7191(1)	19(1)
C(31)	8839(4)	−1312(2)	6109(4)	20(1)
C(32)	8762(4)	−1900(3)	5870(4)	28(1)
C(33)	8290(5)	−2067(3)	5006(4)	36(2)
C(34)	7912(5)	−1655(3)	4372(4)	38(2)
C(35)	8007(4)	−1070(3)	4592(4)	30(1)
C(36)	8460(4)	−896(3)	5451(4)	27(1)
C(41)	9509(4)	−1631(2)	8011(4)	21(1)
C(42)	10294(4)	−1659(3)	8771(4)	28(1)
C(43)	10273(5)	−2066(3)	9440(4)	38(2)
C(44)	9470(5)	−2447(3)	9357(4)	37(2)
C(45)	8695(5)	−2430(3)	8609(5)	34(2)
C(46)	8715(5)	−2026(2)	7941(4)	26(1)
C(5)	8887(4)	−417(2)	7527(4)	20(1)
P(2)	7600(1)	−374(1)	7737(1)	18(1)
C(51)	7554(4)	−868(2)	8660(4)	21(1)
C(52)	8399(5)	−912(3)	9354(4)	29(1)
C(53)	8379(6)	−1250(3)	10097(4)	40(2)
C(54)	7517(6)	−1538(3)	10153(5)	44(2)
C(55)	6666(5)	−1487(3)	9488(5)	41(2)
C(56)	6674(5)	−1149(3)	8725(4)	30(2)
C(61)	6795(4)	−667(2)	6729(4)	22(1)
C(62)	6565(4)	−1259(3)	6634(4)	28(1)
C(63)	6042(5)	−1481(3)	5829(4)	34(2)
C(64)	5737(5)	−1114(3)	5107(5)	37(2)
C(65)	5940(4)	−523(3)	5189(4)	35(2)
C(66)	6459(4)	−293(3)	6002(4)	27(1)
C(71)	9813(11)	2022(7)	7016(8)	175(9)
Cl(71)	10628(2)	1426(2)	7494(2)	95(1)
Cl(72)	9044(3)	2203(2)	7733(4)	167(2)

[a] Equivalent isotropic U defined as one-third of the trace of the orthogonalised U_{ij} tensor.

4.3. Reactions of $[Ru(CO)_2(MeC{\equiv}CPh)(\eta^5\text{-}7,8\text{-}C_2B_9H_{11})]$

(a) A CH_2Cl_2 (15 cm^3) solution of **3c** (0.07 g, 0.17 mmol) was cooled to −95°C and PEt_3 (25 μl, 0.17 mmol) added. After warming to r.t., changes in the yellow mixture were followed by IR spectroscopy in the ν_{max} (CO) region. The reaction was complete after ca. 60 min. The yellow solution was pumped dry in vacuo and the residue crystallised from CH_2Cl_2–*n*-pentane (1:2, 5 cm^3) to afford pale yellow crystals of $[Ru\{C(Me){=}C(Ph)PEt_3\}(CO)_2(\eta^5\text{-}7,8\text{-}C_2B_9H_{11})]$ (**4b**) (0.08 g).

(b) In a similar manner, compound **3c** (0.06 g, 0.16 mmol) in CH_2Cl_2 (15 cm^3) was treated with $Ph_2PCH_2PPh_2$ (0.06 g, 0.16 mmol). Reaction was complete after ca. 45 min. and crystallisation of the yellow solid obtained from CH_2Cl_2–*n*-pentane (1:2, 5 cm^3) yielded pale yellow microcrystals of $[Ru\{C(Me){=}C(Ph)P(Ph)_2CH_2PPh_2\}(CO)_2(\eta^5\text{-}7,8\text{-}C_2B_9H_{11})]$ (**4c**) (0.10 g).

(c) Complex **3c** (0.06 g, 0.14 mmol) in CH_2Cl_2 (15 cm^3) was treated with $AsPh_3$ (0.05 g, 0.15 mmol) and the mixture stirred for 45 min, thereby affording, after removal of solvent in vacuo and crystallisation from CH_2Cl_2–*n*-pentane (1:2, 5 cm^3), off-white crystals of $[Ru(CO)_2(AsPh_3)(\eta^5\text{-}7,8\text{-}C_2B_9H_{11})]$ (**5a**) (0.08 g).

(d) The compound $[Ru(CO)_2(SbPh_3)(\eta^5\text{-}7,8\text{-}C_2B_9H_{11})]$ (**5b**) (0.08 g) was similarly obtained as pale yellow crystals employing **3c** (0.06 g, 0.14 mmol) and $SbPh_3$ (0.05 g, 0.14 mmol).

(e) Compound **3c** (0.07 g, 0.17 mmol) in CH_2Cl_2 (15 cm^3) with $Ph_2P(S)CH_2P(S)Ph_2$ (0.08 g, 0.17 mmol) gave a yellow solution which, after 45 min, was reduced in vacuo to ca. 5 cm^3. Addition of *n*-pentane (10 cm^3) followed by cooling to ca. −20°C afforded yellow crystals of $[Ru(CO)_2\{Ph_2P(S)CH_2P(S)Ph_2\}(\eta^5\text{-}7,8\text{-}C_2B_9H_{11})]$ (**5c**) (0.08 g).

4.4. Synthesis of $[Ru_2(\mu\text{-}Ph_2PCH_2PPh_2)(CO)_4(\eta^5\text{-}7,8\text{-}C_2B_9H_{11})_2]$

(a) A solution of $[NEt_4][RuI(CO)_2(\eta^5\text{-}7,8\text{-}C_2B_9H_{11})]$ (0.11 g, 0.20 mmol) in CH_2Cl_2 (15 cm^3) after addition of $AgBF_4$ (0.04 g, 0.22 mmol) was cooled to −95°C and compound **4c** (0.15 g, 0.19 mmol) was added. The mixture was slowly warmed to r.t. and after stirring for 30 min, it was filtered through Celite and solvent was reduced in volume in vacuo to ca. 5 cm^3. Addition of *n*-pentane (10 cm^3) followed by cooling to −20°C gave yellow crystals of $[Ru_2(\mu\text{-}Ph_2PCH_2PPh_2)(CO)_4(\eta^5\text{-}7,8\text{-}C_2B_9H_{11})_2]$ (**6**) (0.07 g) which were washed with *n*-pentane and dried in vacuo.

(b) To $[NEt_4][RuI(CO)_2(\eta^5\text{-}7,8\text{-}C_2B_9H_{11})]$ (0.20 g, 0.37 mmol) in CH_2Cl_2 (15 cm^3) was added $AgBF_4$ (0.09

g, 0.46 mmol) and the mixture was cooled to −95°C. The phosphine $Ph_2PCH_2PPh_2$ (0.07 g, 0.19 mmol) was added and the mixture allowed to warm to r.t. and then stirred for a further 30 min. The suspension was filtered through Celite and the filtrate reduced in volume in vacuo to ca. 4 cm^3 and chromatographed. Elution with CH_2Cl_2–*n*-pentane (1:1) removed a yellow fraction. Removal of solvent in vacuo gave yellow crystals of $[Ru_2(\mu\text{-}Ph_2PCH_2PPh_2)(CO)_4(\eta^5\text{-}7,8\text{-}C_2B_9H_{11})_2]$ (**6**) (0.16 g) which were washed with *n*-pentane and dried in vacuo.

4.5. X-ray structural analyses

Crystals of **3c**, **4b** and **6** were grown by diffusion of *n*-pentane into CH_2Cl_2 solutions of the complexes. The crystals were mounted on glass fibres and low temperature data were collected on a Siemens SMART CCD area-detector three-circle diffractometer using Mo–K_α X-radiation, $\lambda = 0.71073$ Å. Crystals of **6** were relatively small and poorly diffracting. In addition, the asymmetric unit in **6** contains one molecule of CH_2Cl_2. For three settings of ϕ, narrow data 'frames' were collected for 0.3° increments in ω. In all cases a total of 1321 frames of data were collected affording rather more than a hemisphere of data. It was confirmed that crystal decay had not taken place during the course of the data collections. The substantial redundancy in data allows empirical absorption corrections to be applied using multiple measurements of equivalent reflections. The data frames were integrated using SAINT [10] and the structures were solved by conventional direct methods. The structures were refined by full-matrix least-squares on all F^2 data using Siemens SHELXTL version 5.03 [10], with anisotropic thermal parameters for all non-hydrogen atoms. All hydrogen atoms were included in calculated positions and allowed to ride on the parent boron or carbon atoms with isotropic thermal parameters ($U_{iso} = 1.2 \times U_{iso\ equiv.}$ of the parent atom except for Me protons where $U_{iso} = 1.5 \times U_{iso\ equiv.}$). All calculations were carried out on Silicon Graphics Iris, Indigo, or Indy computers. Experimental data are recorded in Table 6 and final atomic positional parameters for non-hydrogen atoms with equivalent isotropic thermal parameters (x, y, z, U(eq)) are listed in Tables 7–9. Atomic co-ordinates, a complete listing of bond lengths and angles, and the thermal parameters have been deposited at the Cambridge Crystallographic Data Centre.

4.6. Molecular orbital calculations

A semi-empirical ZINDO molecular orbital calculation was carried out using INDO1 parameters with atomic co-ordinates taken from the X-ray crystal structure determination on **3c**.

Acknowledgements

We thank the Robert A. Welch Foundation for support (Grant AA-1201).

References

[1] (a) S. Anderson, D.F. Mullica, E.L Sappenfield, F.G.A. Stone, Organometallics 14 (1995) 3516. (b) S. Anderson, D.F. Mullica, E.L. Sappenfield, F.G.A. Stone, Organometallics 15 (1996) 1676. (c) S. Anderson, J.C. Jeffery, Y-H. Liao, D.F. Mullica, E.L. Sappenfield, F.G.A. Stone, Organometallics 16 (1997) 958.
[2] A.G. Orpen, L. Brammer, F.H. Allen, O. Kennard, D.G. Watson, R. Taylor, J. Chem. Soc. Dalton Trans. (1989) S1.
[3] (a) S.D. Ittel, J.A. Ibers, Adv. Organomet. Chem. 14 (1976) 33. (b) J.L. Templeton, Adv. Organomet. Chem. 29 (1989) 1.
[4] L.E. Smart, J. Chem. Soc. Dalton Trans. (1976) 390.
[5] (a) K.A. Mead, I. Moore, F.G.A. Stone, P. Woodward, J. Chem. Soc. Dalton Trans. (1983) 2083. (b) M.R. Awang, J.C. Jeffery, F.G.A. Stone, J. Chem. Soc. Dalton Trans. (1983) 2091.
[6] ZINDO, CAChe Molecular Modelling package, Oxford Molecular, Oxford, UK.
[7] (a) M.H. Chisholm, H.C. Clark, Acc. Chem. Res. 3 (1973) 202. (b) D.L. Reger, K.A. Belmore, E. Mintz, N.G. Charles, E.A.H. Griffith, E.L. Amma, Organometallics 2 (1983) 101. (c) D.L. Reger, K.A. Belmore, E. Mintz, P.J. McElligott, Organometallics 3 (1984) 134.
[8] Y.-H. Liao, D.F. Mullica, E.L. Sappenfield, F.G.A. Stone, Organometallics 15 (1996) 5102.
[9] C.J. Carmalt, A.H. Cowley, A. Decken, Y.G. Lawson, N.C. Norman, Acta Crystallogr. C52 (1996) 931.
[10] Siemens X-ray Instruments, Madison, WI (1995).